Characterization of Pauci-Chain Polystyrene Microlatex Particles Prepared by Chemical Initiator

Chi Wu,*,† Kam Kwong Chan,† Ka Fai Woo,† Renyuan Qian,‡ Xinhui Li,‡ Liusheng Chen,‡ Donald H. Napper,§ Guilan Tan,§ and Anita J. Hill||

Department of Chemistry, The Chinese University of Hong Kong, Shatin, N. T., Hong Kong, Institute of Chemistry, Academia Sinica, Beijing 100080, China, School of Chemistry, The University of Sydney, Sydney, NSW 2006, Australia, and Faculty of Engineering, Monash University, Clayton, Melbourne, Victoria 3168, Australia

Received May 10, 1994; Revised Manuscript Received December 2, 1994⊗

ABSTRACT: Pauci-chain polystyrene (PCPS) particles, each containing a few polystyrene chains, were prepared by microemulsion polymerization using a chemical initiator. Laser light scattering (LLS), including the angular dependence of the absolute integrated scattered intensity (static LLS) and of the line-width distribution (dynamic LLS), together with fluorescence, positron annihilation lifetime spectroscopy (PALS), and porosimetry, was used to characterize PCPS both in dispersion and as PCPS glasses. The fluorescence spectra showed that ~1% of monomer styrene exists in the PCPS. The LLS results suggest that, on average, one PCPS particle prepared using chemical initiator was composed of only ~6 PS chains confined to the very small volume of the particle (~1000 nm^3). PALS studies showed that the average radius of the free volume cavities inside PCPS is larger than that found in conventional PS latex or bulk PS. The density of PCPS (0.95 g/cm^3) obtained from porosimetry is 9.5% lower than both that of conventional PS latex and bulk PS (1.05 g/cm^3). The density and PALS free volume results suggest that the average intermolecular distance between the segments of the many different interpenetrating polymer chains in bulk or conventional latex PS is smaller than that in PCPS, even though the PS chains in PCPS were confined to a very small volume. This implies that the intersegmental approach inside PCPS was more difficult than that inside a conventional PS latex or bulk PS.

Introduction

Guo *et al.*[1] showed that it is possible to prepare polystyrene microlatex particles (pauci-chain polystyrene (PCPS) particles) which contain only one or at most a few high molecular weight polymer chains by the free radical polymerization of styrene in microemulsions. In the formation of a conventional multichain PS latex (MCPS) or bulk PS, the polymer chain conformation is most likely controlled by thermodynamics. In contrast, the PS chain conformations in PCPS are most likely controlled by the formation kinetics.[2]

Both scaling theory[3] and small angle neutron scattering results[4,5] demonstrate that polymer chains in an amorphous bulk polymer have the same random coil dimensions as in a Θ-solvent. On average, a random coil chain in a bulk polymer occupies only a few percent of its total accessible space. As state by de Gennes,[3] the random coil conformation requires the presence of the order of $N^{1/2}$ interpenetrating polymer chains (where N is the degree of polymerization) to fill the available space. $N^{1/2}$ can be of the order of 100 for a high molecular weight polymer chain.

For PCPS, the particle volume (~1000 nm^3) is much smaller than the accessible volume for a random coil chain in a bulk polymer (~100 000 nm^3). Hence the chains inside PCPS must adopt a compact conformation during the process of chain growth. Since chain packing affects free volume, and hence physical and mechanical properties, it is of interest to compare PCPS with MCPS and bulk PS.

Qian *et al.*[2] showed that for microlatex particles prepared by γ-ray initiation, there is a dramatic difference between PCPS and bulk PS in the first differential scanning calorimetry (DSC) scan of the samples: namely, the existence of a first-order-like exothermic peak that appeared several degrees higher than T_g for PCPS. This exothermic peak was related to the formation of cohesional entanglements that are in addition to the topological entanglements usually considered.[6] This shows that the compact globular form of the PS chains in PCPS at room temperature has a higher conformational temperature than that in bulk PS, where the conformation temperature refers to the temperature at which a multichain sample would exhibit the same ratio of backbone trans to gauche conformations as the single chain sample.

Since the dimensions of a PCPS particle are much smaller than the accessible space of a polymer chain with the random coil conformation in a bulk polymer, it might at first sight be thought that the density of PCPS should be higher than that of the bulk polymer. However, more careful consideration leads to the realization that this speculation may not be correct since the accessible space of a polymer chain with the random coil conformation in a bulk polymer contains on the order of $N^{1/2}$ polymer chains while a PCPS particle contains only a few PS chains. If the intersegmental approach inside PCPS is more difficult than that inside MCPS or bulk PS, the opposite conclusion is reached; i.e., the density of PCPS should be less than that of MCPS or bulk PS. The present work was designed to address this question of chain packing and density and to reveal possible differences between PCPS and MCPS or bulk PS.

Basic Theories

Static Light Scattering. The angular dependence of the excess absolute time-averaged scattered intensity, known as the excess Rayleigh ratio [$R_{vv}(\theta)$], was measured. For a dilute solution or dispersion at concentra-

† Chinese University of Hong Kong.
‡ Academia Sinica.
§ University of Sydney.
|| Monash University.
⊗ Abstract published in *Advance ACS Abstracts,* January 15, 1995.

0024-9297/95/2228-1592$09.00/0

tion C (g/mL) and scattering angle θ, $R_{vv}(\theta)$ can be approximately expressed as[7]

$$\frac{KC}{R_{vv}(\theta)} \cong \frac{1}{M_w}\left(1 + \frac{1}{3}\langle R_g^2\rangle q^2\right) + 2A_2C \quad (1)$$

where $K = 4\pi^2 n^2 (dn/dC)^2/(N_A\lambda_0^4)$ and $q = 4\pi n/\lambda_0 \times \sin(\theta/2)$ with N_A, dn/dC, n, and λ_0 being Avogadro's number, the specific refractive index increment, the solvent refractive index, and the wavelength of light in vacuo, respectively. M_w is the weight average molar mass of the dissolved polymers or suspended particles; A_2, the second virial coefficient; and $\langle R_g^2\rangle_z^{1/2}$ or simply R_g, the root-mean-square z-average radius of gyration of polymer chains or particles. By measuring $R_{vv}(\theta)$ at a set of C and θ, M_w, R_g, and A_2 can be determined from a Zimm plot.[7,8]

Dynamic Light Scattering. An intensity–intensity time correlation function $G^{(2)}(n\Delta\tau,\theta)$ in the self-beating mode is measured, which has the following form[8,9]

$$G^{(2)}(n\Delta\tau,\theta) = \langle I(n\Delta\tau,\theta)I(0,\theta)\rangle = A[1 + \beta|g^{(1)}(n\Delta\tau,\theta)|^2] \quad (2)$$

where A is a measured baseline, β is a parameter depending on the coherence of the detection, n is the channel number, $\Delta\tau$ is the sampling time, and $g^{(1)}(n\Delta\tau,\theta)$ is the normalized first-order electric field time correlation function. For samples with a broad distribution, $g^{(1)}(n\Delta\tau,\theta)$ can be related to the line-width distribution $G(\Gamma)$ by

$$g^{(1)}(n\Delta\tau,\theta) = \langle E(n\Delta\tau,\theta)E^*(0,\theta)\rangle = \int_0^\infty G(\Gamma)e^{-\Gamma n\Delta\tau}\,d\Gamma \quad (3)$$

The analysis program CONTIN[10] was used in the present work to calculate $G(\Gamma)$ from the measured $G^{(2)}(n\Delta\tau,\theta)$. Γ depends on both C and θ.[11] Γ can be related to the translational diffusion coefficient D by $\Gamma = Dq^2$. D can be further related to the hydrodynamic radius R_h by the Stokes–Einstein equation, $R_h = k_BT/(6\pi\eta D)$ where k_B, T, and η are the Boltzmann constant, the absolute temperature, and the solvent viscosity, respectively.

Positron Annihilation Lifetime Spectroscopy (PALS). PALS provides an atomic scale probe which can be used to gain information on the free volume in polymers.[12,13] The free volume sites probed by PALS are cavities which range in diameter from approximately 0.4 to 1.2 nm. As nonbonded interatomic spacings in polymers are typically 0.2–0.6 nm, PALS allows examination of the intra- and intermolecular free volume as well as the free volume at the chain ends. Free volume in polymers consists of dynamic and static components. The ability of PALS to measure both static and dynamic free volume has been demonstrated previously, and further discussion of PALS application to polymers can be found elsewhere.[14,15] PALS spectra in polymers typically consist of three lifetime components; however, in this work it is the third component (τ_3, I_3) which is attributed to the orthoPositronium (oPs) pickoff annihilation in the free volume. The lifetime τ_3 is the inverse of the annihilation rate of oPs by electron pickoff in free volume cavities in the polymer; the intensity, I_3, is a measure of the number of annihilations taking place with the lifetime τ_3. The free volume model of Brandt *et al.*[16] for oPs pickoff annihilation predicts that the lifetime of oPs localized in a free volume cavity is a function of the probability of overlap of the oPs wave function with the wave function of electrons at the cavity wall. The larger the free volume cavity, the longer the oPs pickoff lifetime; therefore, the lifetime, τ_3, can be interpreted as an indication of mean free volume cavity radius. The intensity, I_3, is a function of the positronium formation probability and the relative number of sites available for oPs localization in the volume of material probed. In the absence of oPs inhibition or enhancement, I_3 can be interpreted as the relative number of free volume cavities in the volume probed.

Experimental Methods

Sample Preparation. The % w/v composition of the microemulsion for preparing PCPS was styrene (1.90), *n*-hexanol (0.95), cetyltrimethylammonium bromide (CTAB) (1.90), and water (95.25). The microemulsion was first prepared by titration at 60 °C and then polymerized at the same temperature by AIBN-initiated polymerization for 20 h. Note that a chemical initiator was used instead of γ-ray initiation used previously.[2] The ordinary multichain polystyrene latex (MCPS) sample was purchased from Seradyn (Indianapolis, IN). The stabilizer (surfactant) was removed by an ion-exchange procedure. The particle radius specified by the supplier is 22 nm, and the particle density is 1.05 g/cm^3, which is the same as the density of bulk PS. All dispersions were prepared by diluting a stock dispersion in a known concentration. The solid PCPS particles were harvested by the addition of methanol (5% w/w), after which the system was allowed to stand for about 0.5 h. This desorbed some of the surfactant from the particle surfaces and induced coagulation of the particles. The resulting polymer aggregates were then filtered off using a Teflon filter, washed three times with methanol, and dried at room temperature for density and PALS measurements.

Laser Light Scattering. A commercial LLS spectrometer (ALV-5000, Langen in Hessen, Germany) was used with an argon-ion laser (Coherent INNOVA 90, operated at 488 nm and 400 mW) as the light source. The primary beam is vertically polarized. In the present setup, the value of β is ~0.85, allowing measurements of very dilute solutions. The details of LLS instrumentation and theory can be found elsewhere.[8] All measurements were performed at 25.0 ± 0.1 °C.

Specific Refractive Index Increment (dn/dC). It is vital in static LLS to have a precise value of dn/dC. Recently, a novel differential refractometer was designed and established at the Chinese University of Hong Kong.[17] In this refractometer, a very small pinhole is illuminated by the laser light and then the illuminated pinhole is imaged to the detector by a lens located in the middle between a position sensitive detector and the pinhole. A divided differential refractometer cuvette is placed just before the lens. The pinhole, the cuvette, the lens, and the detector are mounted on a small optic rail. The refractometer can be easily incorporated into any existing LLS spectrometer, wherein the laser, the thermostat, and the computer are shared. Measurements of the refractive index increment and the scattered light intensity under identical experimental conditions, such as wavelength and temperature, can be performed.

Density Determination. The density of the harvested PCPS was determined by Hg porosimetry in a Carlo Erba Porosimeter Po-4000 at room temperature. The dilatometer volume was 15 cm^3 with a 100 mm capillary of 1.5 mm radius. Pressure up to 3.6 kbar could be applied. A sample mass of 0.3506 g was used.

Fluorescence Measurement. For PCPS in a polymerized microemulsion and the PCPS glass particles harvested by methanol washing, fluorescence emission spectra were recorded on a Hitachi F-3000 fluorescence spectrophotometer by 260 nm excitation with both excitation and emission slits set at 5 nm.

PALS Measurements. Spectra were collected in air at 22 °C using an automated EG&G Ortec fast-fast coincidence

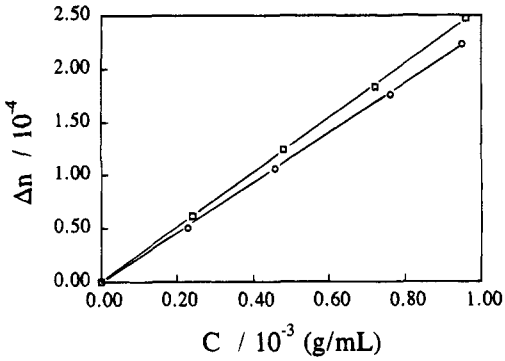

Figure 1. Typical plot of refractive index increment (Δn) versus concentration (C) for PCPS (○) and MCPS (□) in H_2O at 25 °C and λ_0 = 488 nm. The specific refractive index increment dn/dC calculated from the least-squares fitting (the lines) for PCPS and MCPS are respectively 0.236 ± 0.001 and 0.256 ± 0.001 mL/g.

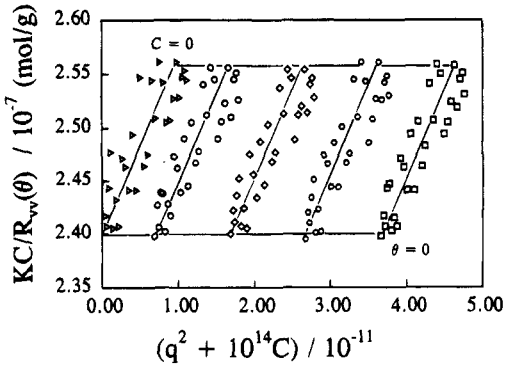

Figure 2. Typical Zimm plot of PCPS in water at 25 °C, where concentration ranges from 1.72 × 10^{-4} to 9.16 × 10^{-4} g/mL.

system with a resolution of 250 ps. A 30 μCi ^{22}Na spot source of 2 mm in diameter was sandwiched between two 2.5 μm thick titanium foil sheets. Polystyrene powder was packed to a depth of 3 mm on both sides of the source sandwich. Ten spectra of 30 000 peak counts were collected for each sample, and population standard deviations were calculated. Each spectra took 2.5 h to collect, and the spectra did not change as a function of contact time with the radioactive source. The spectra were analyzed using PFPOSFIT[18] with a fixed lifetime of 125 ps for τ_1. There was no significant source contribution based on a single lifetime (166 ps) best fit for 99.99% pure annealed and chemically polished aluminum samples.

Results and Discussion

Refractive Index. Figure 1 shows a typical plot of the refractive index increment (Δn) versus concentration (C) for PCPS (○) and MCPS (□) in water at 25 °C and λ_0 = 488 nm. The least-squares fitting results are represented by the lines. The accuracy and stability of the refractometer is so high that we are able to obtain the correct refractive index increment from the measurement of only one concentration.[17] The measured dn/dC for MCPS is 0.256 mL/g which is identical to the literature value,[19] but the measured dn/dC for PCPS is only 0.236 mL/g. The relatively smaller dn/dC value is in accord with the lower density of PCPS.

Light Scattering. Figure 2 shows a typical Zimm plot of PCPS in water at 25 °C, where concentration ranges from 1.72 × 10^{-4} to 9.16 × 10^{-4} g/mL. The data presented in Figure 2 appear very noisy. In fact, close examination of the ordinate scale in Figure 2 shows that the noise is relatively small (less than 2%). The dependence of $KC/R_{vv}(\theta)$ at θ = 0° on C is practically zero (of the order -10^{-7} mol·mL/g^2) for both PCPS and MCPS. In addition to the measurement of PCPS in a microemulsion, the PS chains in PCPS were measured by dissolving the harvested PCPS glass particles in toluene, i.e., the polystyrene solution. The values of M_w and R_g for PCPS, MCPS, and the PS are listed in Table 1. The weight average particle molar mass (M_w) of PCPS is ~6 times of that of one polystyrene chain in PCPS, which shows that on average *each* PCPS particle is composed of about six PS chains. These results show that chemically initiated microlatex particles contain polymer chains of a molecular weight lower than those of γ-initiated particles and so contain more chains per particle. Hereafter, the PCPS studied in this work is denoted as 6CPS. Note that this 6CPS showed an exothermic peak around 109 °C on the first DSC run,[20] as reported previously for single chain PS glasses.[2]

Table 1. Summary of Both Static and Dynamic LLS Results[a]

sample	solvent	dn/dC, mL/g	M_w, g/mol	R_g, nm	$10^7\bar{D}$, cm^2/s	$\bar{R}_h$, nm	$\mu_2/\bar{\Gamma}^2$
PCPS	H_2O	0.236	4.2 × 10^6	12.5	1.53	16.0	0.07
MCPS	H_2O	0.256	2.9 × 10^7	17.1	1.04	23.3	0.05
PS[b]	toluene	0.110	6.6 × 10^5	49.5	1.39	28.5	0.08

[a] Relative errors: dn/dC, ±1%; M_w, ±3%; R_g, ±6%; D, ±1%. [b] PS: polystyrene harvested from the PCPS microlatex particles by adding methanol.

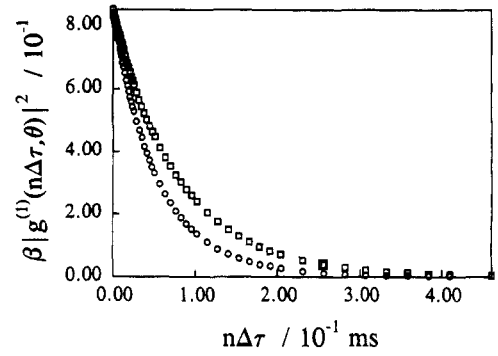

Figure 3. Typical measured intensity–intensity time correlation function of 6CPS (○, C = 1.72 × 10^{-4} g/mL) and MCPS (□, C = 2.14 × 10^{-4} g/mL) at θ = 90° and T = 25 °C.

Figure 3 shows two typical measured intensity–intensity time correlation functions for 6CPS (○) and for MCPS (□). For a sample with a narrow distribution, the measured correlation function can be analyzed by using either the Laplace inversion method, first to obtain $G(\Gamma)$ and then to calculate the z-average line width $\bar{\Gamma}$ (= $\int_0^\infty G(\Gamma)\,\Gamma\,d\Gamma$) and μ_2 (= $\int_0^\infty G(\Gamma)\,(\Gamma-\bar{\Gamma})^2\,d\Gamma$), or the cumulants method to obtain $\bar{\Gamma}$ and μ_2 directly.

Figures 4 and 5 show two typical plots of $\bar{R}_h$ vs θ and C, respectively, where $\bar{R}_h$ was calculated from $\bar{\Gamma}$ with $\bar{\Gamma} = \bar{D}q^2$ by the Stokes–Einstein equation. It can be seen in Figures 4 and 5 that $\bar{R}_h$ depends neither on θ nor on C. This lack of dependence is expected since the average size of these particles was relatively small and the microlatex concentrations were very dilute. The ratios of $R_g/\bar{R}_h$ for both 6CPS and MCPS are close to the value (0.77) predicted for a hard sphere. The values of $\bar{D}$, $\bar{R}_h$, and $\mu_2/\bar{\Gamma}$ (the distribution width of $G(\Gamma)$) are summarized in Table 1. It should be noted that the distribution width of polystyrene in 6CPS is unusually narrow for polymers made from a free radical polymerization. This finding may suggest a way to prepare polymers with a narrow distribution. The values of R_g and $\bar{R}_h$ of the polystyrene dissolved in toluene show that the polymer chains are much more extended (by a factor of 4) in solution compared with those in the particles.

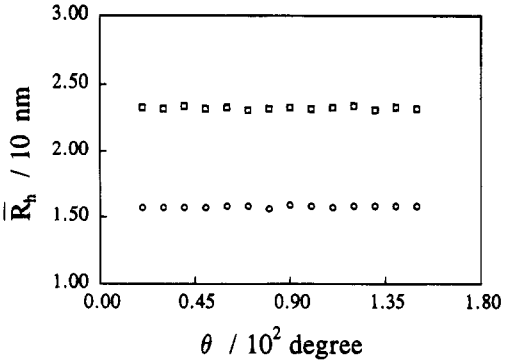

Figure 4. Angular dependence of the z-average hydrodynamic radius $\bar{R}_h$ where $T = 25$ °C and $C = 0$.

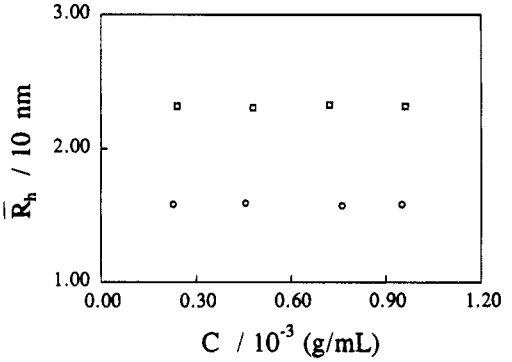

Figure 5. Concentration dependence of the z-average hydrodynamic radius $\bar{R}_h$ where $T = 25$ °C and $\theta = 0°$.

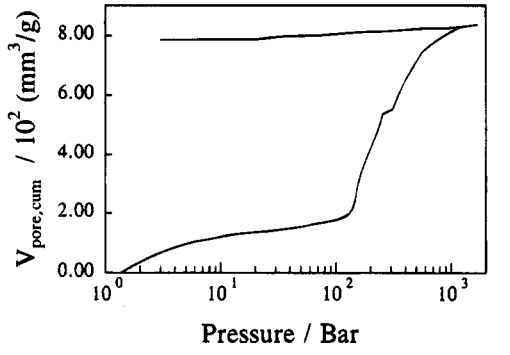

Figure 6. Typical porosimetry result of cumulative pore volume ($V_{pore,cum}$) versus pressure. The lower line is that observed on increasing the pressure, the upper on pressure release.

Porosimetry. Figure 6 shows the results of the porosimetry measurements. The pore volume signifies the interparticle space and space between particle aggregates. From Figure 6 it is easy to assign the pore volume penetrated by Hg under pressures up to 10^2 bar as the space between aggregates, while the pore volume penetrated by Hg at higher pressures is the interparticle space. Above 1.8 kbar the pore volume remained constant. On releasing the pressure some expansion of the true sample volume could be observed, as shown in Figure 6, which was the result of reversible volume elasticity (compressibility) of the sample. The true volume of the 6CPS particles of the sample corrected for the compressibility at 1.8 kbar was 369 mm^3 (correction amounts to −4.5%). Thus the true density of 6CPS particles was 0.95 g/cm^3 which is 9.5% lower than the density of bulk polystyrene (1.05 g/cm^3). This lower density shows that on average the intersegmental distance within 6CPS is larger than that in both ordinary latex particles and bulk polymer.

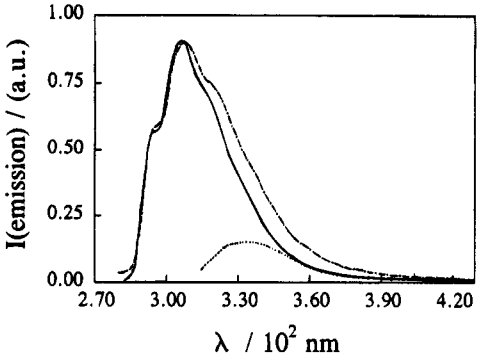

Figure 7. Fluorescence emission spectra of styrene monomer (—) and the 6CPS microemulsion (— · —). $\lambda_{excit} = 260$ nm. The dotted curve is the difference spectrum between the 6CPS microemulsion and styrene monomer.

Table 2. Summary of PALS Results

material	τ_3, ns	I_3, %	R^a
PCPS (6CPS)	2.37 ± 0.02	18.5 ± 0.2	3.2
MCPS (conventional latex)	2.14 ± 0.02	16.8 ± 0.2	3.0
bulk PS (atactic, $M_w = 3 \times 10^5$)[a]	2.07 ± 0.02	(46 − 42)[b]	2.9

[a] Data taken from ref 23. [b] Changes as a function of time.

Fluorescence. Figure 7 shows two typical fluorescence spectra of monomer styrene (—) and 6CPS in microlatex (— · —). The spectra are slightly different. It was found that the fluorescence spectrum of the harvested 6CPS particles by surface reflection is the same as that of bulk polystyrene (not shown). The difference spectra between 6CPS in the microlatex form and styrene monomer shown by the dotted line in Figure 7 is not due to the surfactant present in the microlatex. Instead, the fluorescence spectrum indicates that in the microemulsion there were residual monomer styrene molecules leftover from polymerization.[21] The amount of the residual monomer styrene is less than 0.7%. Due to the much higher quantum efficiency of the styrene fluorescence than of the excimer fluorescence of polystyrene, the latter was masked by the former. The conclusion is that there is still some styrene monomer remaining in the microlatex. During harvesting and washing, the styrene monomer in the 6CPS particles was removed.

PALS. The PALS results are shown in Table 2. The standard deviations are population standard deviations for ten spectra. The results indicate that 6CPS glass particles isolated by the methanol washing have a significantly longer oPs pickoff lifetime, τ_3, than the conventional latex or bulk. As mentioned in the Basic Theory, the PALS parameter τ_3 gives an indication of the mean free volume cavity radius R. Using the theory of Nakanishi *et al.*,[22] the value of τ_3 can be related to the average radius R by

$$\tau_3 = \frac{1}{2}\left[1 - \frac{R}{R+\Delta R} + \frac{1}{2\pi}\sin\left(\frac{2\pi R}{R+\Delta R}\right)\right]^{-1} \quad (4)$$

where τ_3 and R are in the units of nanosecond (ns) and angstroms (Å), respectively, and ΔR (=1.66 Å) is the electron layer thickness. If the free volume cavity is assumed to be spherical, the mean free volume cavity in 6CPS is 137 $Å^3$ compared to 113 and 102 $Å^3$ for MCPS and bulk PS, respectively. The larger mean free volume cavity radius in 6CPS suggests that the packing of the chains in pauci-chain glass is less dense than that found in conventional latex multichain glass.

In polymeric glass the free volume cavities probed by PALS are thought to be located inter- and intrachain

and at chain ends. In addition to the mean size of the free volume cavities, the relative number of free volume cavities is an important parameter. The PALS parameter I_3 gives an indication of the relative number of free volume cavities in the volume probed. Because I_3 is also a function of the positronium (Ps) formation probability, one must ensure that neither Ps inhibition nor enhancement is affecting the value of I_3 if it is to be interpreted in terms of free volume concentration. Sample contact time with the radioactive source has been known to affect I_3 but not τ_3 in bulk PS and other bulk polymers.[23-26] As stated in the Experimental Methods, the τ_3 and I_3 parameters did not change as a function of contact time with the source for the powder samples in this work. However, for the bulk PS quoted in Table 2, the value of I_3 decreased from 46% to 42% as a function of contact time.[23] Two models exist for the formation of Ps: the spur model[27] and the Ore gap model.[28] Both models rely on the availability of suitable electrons to bind with suitable positrons to form positronium (a positron–electron bound state). If the electrons or positrons are scavenged or solvated, then the probability of Ps formation decreases (hence in polymers I_3 decrease). The cause of oPs inhibition in bulk PS has been postulated to be due to chemical inhibition or charging.[24,25] It is likely that the reduced solids content of the powder, as compared to the bulk PS samples, avoids the buildup of charge or the chemical inhibitor which results in the Ps inhibition caused by source contact time in bulk PS. The reduced solids content of the powder also will have another effect on the magnitude of the measured I_3. If there is no Ps inhibition or enhancement, the value of I_3 reflects the relative number of free volume cavities in the volume probed. The amount of solid in the volume probed by PALS will be 2–4 times less in the particulate (powder) PS (i.e., 6CPS and MCPS) samples than in bulk PS, depending on how well the powder is hand-packed around the source. Hence the relative number of free volume cavities (I_3) can be expected to be proportionately less in the powder samples than in bulk samples. The I_3 values of 18.5% and 16.8% are 2.5 and 2.7 times less than the value of 46% in the bulk PS. The lower values of I_3 in the powder samples are most likely due to the reduction of solid-containing PS chains in the volume probed (approximately 1 mm^3). Hence a discussion of I_3 in terms of the relative number of free volume cavities will not be possible until bulk samples are fabricated from the 6CPS and MCPS particles. Baronowski *et al.*[29] have shown that a compaction pressure of 3 tons is sufficient to press disks from latex PS powder which give I_3 values of 36.6% to 39.6%, comparable to bulk PS. The samples in the present study were only lightly compacted by hand with a spatula. An investigation of I_3 in bulk samples pressed or molded from 6CPS and MCPS is planned for future work.

Recent publications[30,31] on the relationship between gas permeability and free volume as measured by PALS have shown a remarkable correlation among τ_3, free volume calculated by the Bondi group contribution method, and gas permeability in glassy and rubbery polymers. In these publications[30,31] the I_3 data were not utilized. Hence even in the absence of comparable I_3 results for all samples, the τ_3 results in the present work strongly support the porosimetry data and the suggestion that the intersegmental dimensions in 6CPS are larger than those in MCPS or bulk PS. This difference in segmental packing may lead to some kinds of applications of PCPS in which transport properties are important.

The data discussed thus far have supported the postulation that the segmental packing in 6CPS differs from that found in conventional PS latex and bulk PS. It has been suggested that the conformations of 6CPS are not typical random coil conformations due to the limited number of interpenetrating polymer chains as well as the limiting particle size. Solid state NMR measurements (^{13}C CPMAS at 5.53 kHz) of 6CPS, conventional PS latex, and bulk PS show identical spectra, supporting the idea that the packing difference is due to conformational differences. As mentioned earlier, the DSC work of Qian *et al.*[5] showing a difference in conformational temperature also supports the postulations put forward in the present work.

Conclusions

The characterization of PCPS has been accomplished by a combination of various methods, including light scattering, fluorescence, porosimetry, and positron annihilation lifetime spectroscopy. We have shown that the present PCPS particles prepared by free radical polymerization of styrene in a microemulsion using a chemical initiator (AIBN) are composed of only six polystyrene chains per particle on average (6CPS). We have experimentally revealed that the density of the 6CPS microlatex particles is 9.5% lower than the density of conventional multichain polystyrene latex (MCPS) and bulk polystyrene. This lower density implies that on average the intersegmental distance within 6CPS is larger than that in both MCPS and bulk polymer. The present study has provided a base for further theoretical study of a single chain, or a few polymer chains, confined inside a limited space. The unique packing of chains in 6CPS as evidenced by the larger free volume cavities may inspire new applications of these specially prepared microlatex particles.

Acknowledgment. Thanks are due to Prof. Guoquan Liu for the use of the Hg porosimeter and to Prof. Xigao Jing for helpful discussions. This project was supported by the Direct Grant for Research 1993/94 of the Chinese University of Hong Kong (No. 220600390) and also partially by the National Basic Research Project of China-Macromolecular Condensed State. The Australian Research Council is thanked for financial support. G.T. gratefully acknowledges the award of an EMSS by the Australian Government. Dr. T. J. Bastow of CSIRO Division of Materials Science and Technology is acknowledged for the solid state NMR work.

References and Notes

(1) Guo, J. S.; El-Aasser, M. S.; Vanderhoff, J. W. *J. Polym. Sci., Polym. Chem. Ed.* **1989**, *27*, 691.
(2) Qian, R.; Wu, L.; Shen, D.; Napper, D. H.; Mann, R. A.; Sangster, D. F. *Macromolecules* **1993**, *26*, 2950.
(3) de Gennes, P.-G. *Scaling Concepts in Polymer Physics*; Cornell University: Ithaca, NY, 1979; Chapter 2.
(4) Kirste, R. G.; Kruse, W. A.; Scheltens, J. *Makromol. Chem.* **1973**, *162*, 299.
(5) Cotton, J. P.; Decker, D.; Benoit, H.; Farnoux, B.; Higgins, J.; Jannink, G.; Ober, R.; Picot, C.; des Cloizeaux, J. *Macromolecules* **1974**, *7*, 863.
(6) Qian, R. *Abstr. China-UK Bilateral Conference on Polymer Science*, Beijing, April 1992; p 2.
(7) Zimm, B. H. *J. Chem. Phys.* **1948**, *16*, 1099.
(8) Chu, B. *Laser Light Scattering*; Academic Press: New York, 1974.

(9) Pecora, R. *Dynamic Light Scattering*; Plenum Press: New York, 1976.
(10) Provencher, S. W. *Biophys. J.* **1976**, *16*, 29; *J. Chem. Phys.* **1976**, *64*, 2772; Makromol. *Chem.* **1979**, *180*, 201.
(11) Stockmayer, W. H.; Schmidt, M. *Pure. Appl. Chem.* **1982**, *54*, 407; *Macromolecules* **1984**, *17*, 509.
(12) Stevens, J. R. *Methods Experimental Phys.* **1980**, *16A*, 371.
(13) Jean, Y. C. *Microchem. J.* **1990**, *42*, 72.
(14) Simon, G. P.; Zipper, M. D.; Hill, A. J. *J. Appl. Polym. Sci.* **1994**, *52*, 1191.
(15) Zipper, M. D.; Hill, A. J. *Mater. Forum* **1994**, *18*, 215.
(16) Brandt, W.; Berko, S.; Walker, W. *Phys. Rev.* **1960**, *120*, 1289.
(17) Chi, Wu.; Xia, K. Q. *Rev. of Sci. Instrum.* **1994**, *65*, 587.
(18) Puff, W. *Comput. Phys. Commun.* **1983**, *30*, 359.
(19) Chan, F. S.; Coring, D. A. I. *Can. J. Chem.* **1966**, *44*, 725.
(20) Tan, G. Unpublished Ph.D. research results.
(21) Bastile, L. J. *J. Chem. Phys.* **1962**, *36*, 2204.
(22) Nakanishi, H.; Wang, S. J.; Jean, Y. C. In *International Symposium on Positron Annihilation Studies in Fluids*; Sharma, S. C., Ed.; World Scientific; Singapore, 1987; p 292.
(23) O'Connor, P. J.; Kocher, C. W.; Landes, B. G.; Anderson, S. L.; Delassus, P. T. Gruike, E. A. *Polym. Prepr. (Am. Chem. Soc., Div. Polym. Chem.)* **1992**, *33*, 308.
(24) Welander, M.; Maurer, F. H. J. *Mater. Sci. Forum* **1992**, *105–110*, 1811.
(25) Li, X.; Boyce, M. *J. Polym. Sci. B* **1993**, *31*, 869.
(26) Hill, A. J.; Zipper, M. D.; Simon, G. P. *Proceedings of the 1st Austral-Asian Conference on Radiation Chemistry and Nuclear Medicine*; AINSE: Sydney, 1993; p 46.
(27) Mogensen, O. E. *J. Chem. Phys.* **1974**, *60*, 998.
(28) Brandt, W. *Appl. Phys.* **1974**, *5*, 1.
(29) Baranowski, A.; Debowski, M.; Jerie, K.; Mirkiewicz, G.; Rudzinska-Girulska, J.; Tadeusz Sikorski, R. *J. Phys. IV* **1993**, *3*, 225.
(30) Kobayashi, Y.; Haraya, K.; Kamiya, Y.; Hattori, S. *Bull. Chem. Soc. Jpn.* **1992**, *65*, 160.
(31) Kobayashi, Y.; Haraya, Y.; Hattori, Sasuga, T. *Polymer* **1994**, *35*, 925.

MA941255Y